Conditional Deletion of AP-2α and AP-2β in the Developing Murine Retina Leads to Altered Amacrine Cell Mosaics and Disrupted Visual Function

Emily Anne Hicks,[1] Mizna Zaveri,[2] Paula A. Deschamps,[2] Michael D. Noseworthy,[1,3,4] Alexander Ball,[2] Trevor Williams,[5] and Judith A. West-Mays[1,2]

[1]McMaster School of Biomedical Engineering, McMaster University, Hamilton, Ontario, Canada
[2]Department of Pathology and Molecular Medicine, McMaster University, Hamilton, Ontario, Canada
[3]Department of Electrical and Computer Engineering, McMaster University, Hamilton, Ontario, Canada
[4]Department of Radiology, McMaster University, Hamilton, Ontario, Canada
[5]Department of Craniofacial Biology and Department of Cell and Developmental Biology, University of Colorado Denver, Anschutz Medical Campus, Aurora, Colorado, United States

Correspondence: Judith A. West-Mays, McMaster University, 1200 Main Street West, HSC 4N67, Hamilton, Ontario L8N 3Z5, Canada; westmayj@mcmaster.ca.

EAH and MZ contributed equally to the work presented here and should therefore be regarded as equivalent authors.

Submitted: November 13, 2017
Accepted: March 27, 2018

Citation: Hicks EA, Zaveri M, Deschamps PA, et al. Conditional deletion of AP-2α and AP-2β in the developing murine retina leads to altered amacrine cell mosaics and disrupted visual function. *Invest Ophthalmol Vis Sci*. 2018;59:2229–2239. https://doi.org/10.1167/iovs.17-23283

Purpose. The combined action of the activating protein-2 (AP-2) transcription factors, AP-2α and AP-2β, is important in early retinal development, specifically in the formation of horizontal cells. However, in previous studies, it was not possible to analyze postnatal development and function of additional retinal subtypes.

Methods. We used a double conditional deletion of AP-2α and AP-2β from the retina to further examine the combinatory role of these genes in retinal cell patterning and function in postnatal adult mice as measured by Voronoi domain area and nearest-neighbor distance spatial analyses and ERGs, respectively.

Results. Conditional deletion of both AP-2α and AP-2β from the retina resulted in a variety of abnormalities, including the absence of horizontal cells, defects in the photoreceptor ribbons in which synapses failed to form, along with evidence of aberrant amacrine cell arrangement. Although no significant changes in amacrine cell population numbers were observed in the double mutants, significant irregularities in the mosaic patterning of amacrine cells was observed as demonstrated by both Voronoi domain areas and nearest-neighbor distances analyses. These changes were further accompanied by an alteration in the retinal response to light as recorded by ERGs. In particular, in the double-mutant mice lacking AP-2α and AP-2β, the b-wave amplitude, representative of interneuron signal processing, was significantly reduced compared with control littermates.

Conclusions. Together these findings demonstrate the requirement for both AP-2α and AP-2β in proper amacrine mosaic patterning and a normal functional light response in the retina.

Keywords: retina development, amacrine cells, horizontal cells, mosaic patterning electroretinograms

The retina is an extension of the central nervous system derived from the forebrain neural ectoderm. In mice, neural retinogenesis commences at embryonic day (E)10.5 and ends at postnatal day (P)11. During these 3 weeks, multipotent retinal progenitor cells (RPCs) give rise to six principal classes of neurons. These cells emerge in a timely and ordered manner, beginning with the genesis of ganglion cells (GCs), followed by horizontal cells (HCs), cone photoreceptors (PRs), amacrine cells (ACs), rod PRs, bipolar cells (BCs), and finally the non-neuronal Müller glia cells.[1] Although environmental signals are able to modify the relative proportions of cell types generated by RPCs at a certain time, these extrinsic influences cannot force RPCs to produce cell types that they were not already competent to generate.[1] Thus, there is increasing evidence for transcription factors as key intrinsic regulators of retinal progenitor maintenance, cell fate determination. and terminal differentiation.[2–4] All mitotic RPCs coexpress a set of transcription factors that includes the homeodomain factors Pax6, Six3, Rx1, and Chx10, and the basic-helix-loop-helix (bHLH) factor Hes1.[2] As retinogenesis progresses, expression of these progenitor factors is maintained in some cell lineages but downregulated in others. Additionally, other transcription factors become expressed in a subset of RPCs, including neurogenic bHLH transcription factors, such as Math5, Mash1, and NeuroD, as well as, Ptf1a,[5,6] Foxn4, and AP-2α, resulting in a different combination of factors that direct the fate and differentiation of each retinal cell type.[5,7]

The activating protein-2 (AP-2) transcription factors are a developmentally important family of genes that our laboratory and others have shown to play important roles in retinogenesis.[8–14] The AP-2 family consists of a class of five different transcription factors: AP-2α, AP-2β, AP-2γ, AP-2δ, and AP-2ε, which form homo- or heterodimers. They bind to target sequences and regulate the transcription of target genes.[15] These proteins have a basic DNA-binding domain that binds to the palindromic consensus sequence 5′-GCCNNNGGC-3′, fol-

lowed by a characteristic helix-span-helix motif that facilitates dimerization and DNA binding, together encoded by exons 4 to 7.[15] In the mouse retina, AP-2α and AP-2β are coexpressed in the embryonic and adult retina, initially in the inner nuclear layer (INL) and a subset of cells in the ganglion cell layer (GCL), both of which correspond to expression in ACs and HCs.[9,10] AP-2γ expression is restricted to ACs, in a subset that is partially distinct from the AP-2α/β-immunopositive population,[9] whereas AP-2δ is expressed in a subset of GCs.[9,14]

A number of loss-of-function and gain-of-function studies in mice have been used to investigate the role of AP-2 genes in retinogenesis.[8–14] Our laboratory first examined *AP-2α* germline knockout (KO) mice that have severe developmental defects, including ocular abnormalities, which involve the optic cup (presumptive retina).[8] However, because these mice die prenatally from severe developmental defects,[16,17] retinogenesis could not be examined beyond birth. As a result, we used Cre-loxP technology to conditionally delete AP-2α from the presumptive retina (*Ret-AP-2α* mice). Detailed examination of these conditional *Ret-AP-2α* mice revealed no detectable abnormalities in the neural retina.[10] Because AP-2α and AP-2β exhibit overlapping expression patterns in the AC and HC populations, we surmised that AP-2β might play a potential compensatory role. To investigate this, we created a mutant model in which the conditional *Ret-AP-2α* mutants were crossed onto an AP-2β germline KO background.[9] This model revealed that in the absence of both AP-2α and AP-2β in the retina, a complete absence of HC was observed and potential defects in AC positioning and homotypic spacing were suspected.[9]

The possible disruption of AC positioning is of particular interest, as these cells have a significant role in specific aspects of visual perception. Retinal mosaics allow visual images to be processed uniformly across the various neurons. AC mosaics are particularly important for extracting visual data related to direction of motion of the ON and OFF visual pathways.[18,19] Retinal mosaic patterning is not well understood, particularly the arrangement of ACs in both the INL and GCL. Thus, the current study further investigates how AP-2α and AP-2β influence AC mosaic formation. Because the previously generated mutant mice did not survive past birth, due to germline deletion of AP-2β, we have generated a new model for conditional deletion of AP-2α and AP-2β from the retina, in which mice survive postnatally (DBL α/β mice). Our findings show that although no significant changes in AC population numbers were observed in the DBL α/β mutants, significant irregularities in the mosaic patterning of ACs as determined by both Voronoi domain areas and nearest-neighbor distances analyses were observed. In addition, an absence of HCs was found, as well as thinning of the outer plexiform layer (OPL) and altered PR synapses. Interestingly, these observed cellular changes resulted in an alteration in the retinal response to light as recorded by ERGs.

Methods

Generation of Mouse Lines

All animal procedures were performed in accordance with the ARVO Statement for the Use of Animals in Ophthalmic and Vision Research. Five mouse lines were used to create αKI (*Tfap2a*$^{ki7lacZ/lox}$), βKO (*Tfap2b*$^{KO/lox}$), or DBL (*Tfap2a*$^{ki7lacZ/lox}$/*Tfap2b*$^{KO/lox}$) KOs. Two *Tfap2* alleles were incorporated into the breeding scheme, including the *Tfap2a*^{ki7lacZ} null allele (due to germline IRES-lacZ knockin insertion disrupting exon 7)[20]; and a *Tfap2b*^{KO} null allele (due to the germline insertion of a PGK-neo cassette disrupting exon 4).[21] *Tfap2a*$^{ki7lacZ/+}$ mice were crossed with α-Cre$^{+/-}$ transgenic mice[22] expressing Cre recombinase under control of the retina-specific "Pax6 α enhancer" from the murine Pax6 gene. When activated at E10.5, this Cre-mediated excision leads to the loss of AP-2α and AP-2β expression in the peripheral retina. α-*Cre*$^{+/-}$/*Tfap2a*$^{ki7lacZ/+}$ mice were then crossed with *Tfap2b*$^{-/+}$ mice to generate mice that had only one functional copy of *Tfap2a* and *Tfap2b*, and retained the expression of the α-Cre transgene. In a second cross, homozygous *Tfap2a*$^{lox/lox}$ mice[23] were bred with mice homozygous for the *Tfap2b*$^{lox/lox}$ allele in which exons 5 and 6 of *Tfap2a* and exon 6 of *Tfap2b* are flanked by single *loxP* sites to obtain *Tfap2a*$^{lox/lox}$/*Tfap2b*$^{lox/lox}$ mice that were homozygous floxed for both alleles. This allows for the second copy of *Tfap2a and Tfap2b* to be conditionally deleted by Cre-mediated excision. The final cross of this breeding scheme is expected to result in only one-eighth of the offspring being conditional DBL mutants (DBL KO). The same *Tfap2* alleles and Cre recombinase were used to create single conditional mutants. In these mating pairs, only one AP-2 family member was deleted, either *Tfap2a* (αKI) or *Tfap2b* (βKO), whereas the other *Tfap2* alleles remained unaltered. For example, α-*Cre*$^{+/-}$ transgenic mice were bred with *Tfap2a*$^{ki7lacZ/+}$ and the resulting offspring, α-*Cre*$^{+/-}$/*Tfap2a*$^{ki7lacZ/+}$ were crossed with homozygous floxed *Tfap2a*$^{lox/lox}$ mice. This breeding scheme allows for the conditional KO of only *Tfap2a* from the retina, while *Tfap2b* remains the same (α-*Cre*$^{+/-}$/*Tfap2a*$^{ki7lacZ/lox}$).

For all genotyping, DNA was extracted from adult ear clips using the EZNA Tissue DNA Kit (Omega Bio-Tek, Norcross, GA, USA). Genotypes were determined by previously established PCR protocols.[9] Littermates used as controls either contained two functional copies of *Tfap2a* and *Tfap2b* in the retina, or were missing one functional copy of either allele if the former was not available.

Histology

Dissected whole eyes were collected from KO mice and control littermates, following euthanasia by CO_2 overdose. Tissue was fixed in 10% neutral buffered formalin (Sigma-Aldrich, Oakville, ON, Canada) for 24 hours then stored in 70% ethanol. Samples were processed (Core Histology Laboratory, McMaster University, Hamilton, ON, Canada) and embedded in paraffin (Paraplast Tissue Embedding Media; Fischer Scientific, Waltham, MA, USA). Serial sections were cut to 4 μm in thickness and used for immunofluorescent analysis or hematoxylin and eosin (H&E) staining.

Immunofluorescence

Indirect immunofluorescence was performed on paraffin sections. Sections were deparaffinized in xylene, hydrated (through 100%, 95%, 75% ethanol, followed by water), treated with 10 mM sodium citrate buffer (pH 6.0; boiling for 20 minutes) for antigen retrieval, blocked with normal goat or donkey serum, and incubated with primary antibodies overnight at 4°C. Primary antibodies included mouse monoclonal anti-AP-2α (3B5) undiluted 1:1 (Developmental Studies Hybridoma Bank, University of Iowa, Iowa City, IA, USA); rabbit polyclonal anti-AP-2β at 1:50 (Cell Signaling Technology, Inc., Danvers, MA, USA); mouse monoclonal anti-β-catenin at 1:100 (BD Biosciences, San Jose, CA, USA); mouse monoclonal anti-calbinin (clone CL-300) at 1:250 (Sigma-Aldrich); goat polyclonal anti-choline acetyltransferase at 1:100 (Millipore Sigma, Etobicoke, ON, Canada); goat polyclonal anti-glycine transporter 1 (anti-GlyT1) at 1:5000 (Millipore-Chemicon, Billerica, MA, USA); rabbit polyclonal anti-γ-aminobutyric acid (GABA) transporter 1 (anti-GAT-1) at 1:250 (Abcam, Cambridge, MA, USA); mouse monoclonal anti-Neurofilament 160 (clone NN18)

at 1:300 (Sigma-Aldrich); rabbit polyclonal anti-onecut-1 at 1:100 (Santa Cruz Biotechnology, Mississauga, ON, Canada); and rabbit polyclonal anti-Sox2 at 1:1000 (Millipore-Chemicon). Appropriate species-specific fluorescent secondary antibodies Alexa Fluor 568 nm or 488 nm (Invitrogen/Molecular Probes, Burlington, ON, Canada) were used 1:200 for 1 hour at room temperature. For all colocalization studies, both primaries and both secondaries were mixed and incubated simultaneously. All slides were mounted with ProLongGold antifade mounting medium with 4,6-diamino-2-phenylindole (DAPI; Vector Laboratories, Burlington, ON, Canada). All sections were visualized with a microscope (Leica, Deerfield, IL, USA) equipped with an immunofluorescent attachment, and images were captured with a high-resolution camera and associated software (Leica Application Suite X; LasX, Deerfield, IL, USA). Images were reproduced for publication with image management software (Photoshop CC 2017; Adobe Systems, Inc., San Jose, CA, USA).

Cell-Counting Studies

To quantify ACs in the different mouse groups, immunolabeled cells in a 600-μm length of retinal section equidistant from the periphery were counted in a minimum of three sections from three different animals and expressed as the mean ± SD. Data were tested for significance by 1-way ANOVA (GraphPad Prism 7; GraphPad Software, San Diego, CA, USA) comparing the different mouse genotypes with a common control. Bonferroni post hoc comparisons were made when statistical significance ($P < 0.05$) was found between observations. A sample size of at least three mutant and three control retinas was used for each strain. Sections closely preceding or following those used for cell counts were previously stained with anti-AP-2α or anti-AP-2β to confirm deletion in these regions.

Flat Mounting Retinas and Voronoi Domain (VD) and Nearest-Neighbor (NN) Analyses

Mouse eyes were removed and fixed for 2 hours in 4% buffered formalin. Retinas were dissected whole, rinsed in PBS, and permeabilized overnight with 0.3% Triton X-100 in PBS (PBST). Next, they were blocked in normal serum for 3 hours at room temperature and transferred to a primary antibody solution containing 1% dimethyl sulfoxide (DMSO) and 5% normal serum in PBST and agitated for 72 hours at 4°C. Subsequently, they were washed in PBST and incubated in Alexa Fluor secondary antibodies (1:200) in PBST with 1% DMSO and 2.5% normal serum for 4 hours at room temperature. Finally, retinas were rinsed in PBS before being flat mounted on clean slides with ProLongGold antifade mounting medium with DAPI.

Flat mount retinas were examined using a ×20 objective on a Leica microscope equipped for fluorescence imaging. Fields were sampled from the peripheral retina, approximately two-thirds from the optic nerve head, in four quadrants, sampling cholinergic amacrine cell mosaics in both the INL and GCL in the eight loci. For each field, VD and NN values were calculated using the FIJI version of ImageJ software (http://imagej.nih.gov/ij/; provided in the public domain by the National Institutes of Health, Bethesda, MD, USA).[19] Threshold values were set for each fluorescent image to isolate immunopositive cells of interest. The image was then converted to binary and the VD plug-in was used. Areas for each bound cell were calculated. The VD area was defined as the area of all points in the plane of the retina closer to that one cell than to any other cells, whereas the NN distances measure how close homotypic cells are in relation to one another. The collection of NN distances and VD areas was then used to calculate a regulatory index (RI), being the average NN or VD divided by its SD. Comparisons were tested for significance with 1-way ANOVA (GraphPad Prism 7). Bonferroni post hoc comparisons were made when statistical significance ($P < 0.05$) was found between treatment groups. For each group, four retinas were analyzed with all values expressed as the mean ± SD.

Electroretinograms

Scoptic full-field ERGs (Ganzfeld ERG; Phoenix Research Laboratories, Pleasanton, CA, USA) were recorded from dark-adapted mice (12 hours) under dim, red light (750 nm). Animals were anesthetized with 2.5% avertin (0.015 mL/mg body weight) intraperitoneally, supplemented as necessary subcutaneously. Pupils were dilated with 0.5% tropicamide and 2.5% phenylephrine hydrochloride ophthalmic solutions (AKORN, Lake Forest, IL, USA). Tear-Gel ophthalmic liquid gel (Alcon Canada, Mississauga, ON, Canada) was applied throughout the procedure to prevent drying of the cornea and to maintain coupling of the corneal electrode.

Animals were place on a heated platform (37°C) with a platinum-plated ground electrode placed in the base of the tail and a platinum reference electrode placed in the scalp, between the ears. The gold-plated corneal electrode was positioned in contact with the Tear-Gel solution on the cornea, completing the circuit. Series of 2-ms, single-flash recordings were obtained using a light-emitting diode stimulus (504 nm) at increasing light intensities (−1.6 to 3.0 $cd{\cdot}s{\cdot}m^{-1}$, on a log scale) with 20 responses recorded for low-level stimuli, to 3 for the highest flash intensities. The interstimulus interval increased from 1 second for low stimuli to 120 seconds for the highest. The a- and b-wave amplitudes of the resulting ERGs were evaluated using associated software (LabScribe; iWork System, Inc., Dover, NH, USA). Three eyes were examined for each group expressed as the mean ± SD. A 2-way repeated-measures ANOVA was performed to analyze the effects of genotype and the repeated light intensity measures on a- and b-wave amplitudes. Post hoc analysis using Tukey's HSD indicated at which light intensities the amplitudes were different between genotypes. Statistical significance was defined as $P < 0.05$.

Electron Microscopy

Before enucleation, eyes were marked with a Davidson dye (Bradley Products, Inc., Cedarlane, Burlington, ON, Canada) to indicate dorsal, nasal, temporal, and ventral regions. The anterior parts of the eyes were then removed, and the neural retinas were separated from the pigment epithelium. The retinas were then quartered into their respective regions: dorsal, nasal, temporal, and ventral. These regions were then fixed by immersion in a primary fixative, 2% paraformaldehyde/2.5% glutaraldehyde, buffered in 0.15 M sodium cacodylate buffer, overnight at 4°C. Retinas were then washed in the same buffer and post fixed in a 1:1 solution of 2% aqueous OsO_4/0.2 M sodium cacodylate buffer for 2 hours at 4°C, and then washed again in the buffer. Retinas were then serially dehydrated in ethanol, and embedded in Spurr's resin in preparation for transmission electron microscopy (TEM) analysis. Thin sections (60–80 nm) were obtained with an ultramicrotome (Reichert-Jung Ultracut E Microtome; American Instruments, Haverhill, MA, USA) using a diamond knife, collected onto copper 75/300 mesh grids (Electron Microscopy Sciences, Hatfield, PA, USA), and stained with 2% (wt/vol) uranyl acetate and Reynolds' lead citrate. Sections were viewed using a JEOL 100CX electron microscope (JEOL USA, Inc., Peabody, MA, USA) at an accelerating voltage of 60 keV, and digital images were collected and stored on a computer for subsequent viewing and analysis.

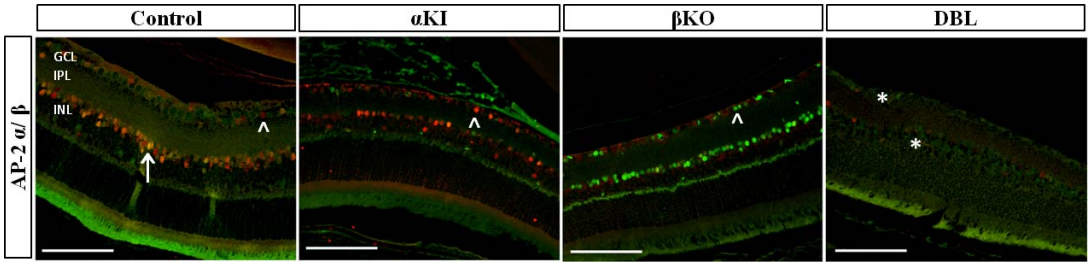

FIGURE 1. Expression of AP-2α/AP-2β in the retina. Immunofluorescent staining of P50 sagittal section of the eye showing AP-2α (*green*) and AP-2β (*red*) exhibit overlapping expression patterns in the adult mouse retina (*arrow*). Both proteins are expressed in the INL where HCs and ACs reside, and they are expressed in displaced ACs in the GCL (*arrowheads*). This expression is completely lost in the AP-2α/β DBL KO (*). Loss of AP-2α expression in αKI and AP-2β in βKO mice did not affect the expression of the other marker. *Scale bars*: 100 μm.

RESULTS

Mice with homozygous global deletion of *Tfap2a* or *Tfap2b* are not viable or die shortly after birth. Thus, to examine retinogenesis through postnatal stages, conditional deletion of *Tcfap2a* (αKI; $Tcfap2a^{ki7lacZ/lox}$), *Tcfap2b* (βKO; $Tcfap2d^{KO/lox}$), or both *Tcfap2a* and *Tcfap2b* (DBL α/β KO; $Tcfap2a^{ki7lacZ/lox}$/$Tcfap2b^{KO/lox}$) from the developing retina was achieved through a Cre-loxP approach using the α-$Cre^{+/-}$ transgenic line.[22] To ensure deletion was successful from the neural retina, AP-2α and AP-2β expression was monitored via immunofluorescence in αKI, βKO, and DBL α/β KO mutants and compared with littermate controls (Fig. 1). AP-2α and AP-2β expression was readily detected in the INL and GCL of control retinas; however, a clear deletion of both was observed in DBL α/β KO retinas. In comparison, single αKI mice demonstrated a loss of AP-2α expression in the INL and GCL, whereas AP-2β expression remained comparable to that of controls. Similarly, in βKO mutants, AP-2β was no longer detected in the INL and GCL, whereas AP-2α expression remained unchanged.

AC Development is Independent of AP-2α and AP-2β Expression

Most ACs in the mammalian retina contain either glycine or GABA inhibitory neurotransmitters, making these the two predominant AC populations with each making up close to half of all ACs.[24] As we have shown previously, the adult retina expresses AP-2α and AP-2β in both the glycinergic and GABAergic AC populations, with a 77% overlap in their expression profiles.[9] Furthermore, we demonstrated that deletion of these two proteins from the embryonic retina did not appear to influence the genesis of ACs.[9] To investigate how loss of these two transcription factors impacted ACs later in retinal development, we examined the AC populations in the adult DBL α/β KO. GABAergic ACs are the first AC population to arise during retinogenesis, followed by glycinergic ACs and a small subset of dopaminergic ACs. Thus, the GABA transporter 1 (GAT-1) is a reliable indicator of mature AC interneurons, labeling their membranes, and was used as a marker in histological sections from single αKI or βKO, and DBL α/β KO mice to examine the effect the deletion of these proteins may have on the GABAergic population of ACs. These studies revealed that there was no significant decrease in GAT-1 immunopositive cells in any of the conditional KO lines when compared with controls (Figs. 2A, 2B), whereas an increase in GAT-1 immunopositive cells was observed in single αKI mice (Figs. 2A, 2B). Cholinergic ACs are one of the earliest-born subsets of the GABAergic population.[25] The transcription factor Sox2, while expressed in RPCs, is a marker for cholinergic ACs and Müller glia.[26] Sox2 immunolabeling also showed no significant changes in the population number of this subset of ACs in any of the mouse KO line retinas sampled (Figs. 2A, 2C). Glycinergic ACs are born later during retinal development, near P0. To determine if the deletion of AP-2α or AP-2β during retinogenesis effects this population of cells in the adult retina, anti-glycine transporter-1 (GLYT-1) was used to stain the membranes of these ACs (Fig. 2D). When compared with control retinas, there were no significant changes observed in any of the conditional KO mice analyzed (Figs. 2A–2D). Thus, examination of several AC markers did not reveal any significant decrease in the number of ACs in any of the single or DBL α/β KO mice.

Cholinergic AC Mosaics Are Altered by Deletion of AP-2α and AP-2β From the Retina

Visual processing relies on the correct arrangement of neurons within the retina. ACs in the INL and GCL are vital for both ON and OFF visual pathways, as they participate in the extraction of the direction of motion with their mosaic fundamental for proper visual processing.[19] In an earlier study from our laboratory, histological sections of embryonic mice lacking AP-2α and AP-2β revealed that although AC population numbers were not significantly affected, their distribution in the INL and GCL was disorganized when compared with controls.[9] This previous examination was limited to histological sections of embryonic retinas, which restricted our ability to accurately determine how the spacing of AC mosaics may have been affected. Thus, to fully characterize cholinergic AC patterning in postnatal single and DBL α/β KO mice, immunofluorescence analyses on whole retinal flat mounts was performed using a cholinergic AC-specific marker, choline acetyltransferase (ChAT), along with AP-2α or AP-2β. Examination of retinal flat mounts revealed that ChAT-positive cell populations in the conditional KO mice exhibited altered patterns compared with control littermates (Fig. 3A). To quantify these differences, we used the preferred methods for examining the regularity of retinal mosaics, the VD areas and NN distances in flat mount retinas.[19] The VD of a cell is the area of all points in the plane of the retina that are closer to that cell than to any other cell, measuring the regularity in the coverage of the retina by these cells. The NN distances determine the proximity of the homotypic cells. The collection of NN distances and VD areas were then divided by their respective SDs to calculate an RI. These studies demonstrated that the NNRI of the INL layer was significantly lower in the DBL α/β KO mice when compared with controls (Fig. 3B), with an average NNRI of 3.12 ± 0.60 in the DBL compared with 4.19 ± 0.39 in the controls ($P < 0.03$). The lower index values reveal greater irregularity. In comparison, neither the single αKI nor βKO retinas displayed a significant difference in NNRI values compared with control littermates. With respect to the NNRI

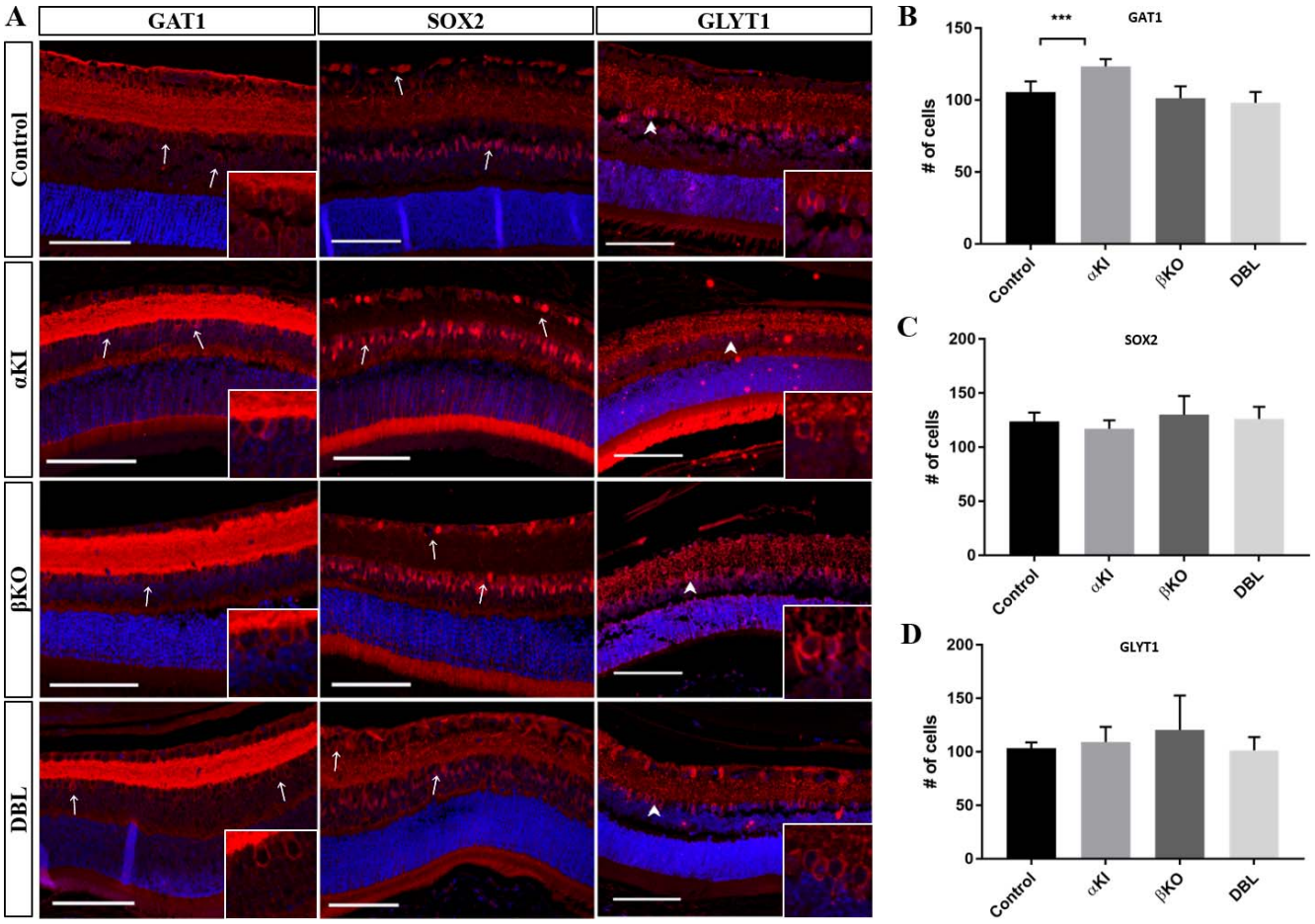

Figure 2. Expression of GABAergic and glycinergic AC markers GAT1, SOX2, and GLYT1. (**A**) Immunofluorescent staining of P50 sagittal sections of the eye showing GAT1 (*red*), a marker for GABAergic AC, showed similar membrane-bound staining in all animals studied (*arrows*). SOX2 (*red*), a marker for the cholinergic subset of GABAergic AC, had similar expression in the conditional KO models to that seen in controls (*arrows*), shown with nuclear stain DAPI (*blue*). GLYT1 (*red*) in AC membranes (*arrowheads*) in the INL and GCL remains unchanged between the various models. Inlays, ×40 magnification. (**B**) A significant increase in GAT1-positive cells was seen in αKI mice (123.0 ± 5.2) compared with controls (106.0 ± 7.4). (**C**) No significant changes were seen in the number of SOX2-positive or (**D**) GLYT1-positive cells in any group ($P > 0.05$). (Mean ± SD for three retinas per group; $^{***}P < 0.0004$, 1-way ANOVA with Bonferroni multiple comparison tests.) *Scale bars*: 100 μm.

in the GCL, no significant difference was observed between any of the conditional KO mouse groups compared with controls (Fig. 3C). Correspondingly, the VDRI was also significantly lower in the INL of DBL α/β KO mice when compared with controls, falling to 1.75 ± 0.38 below 3.38 ± 0.68 ($P < 0.01$) in controls (Fig. 3D). Again, no significant difference was observed for the VDRI of the GCL between the conditional KO mice and controls (Fig. 3E). Interestingly, the NNRI and VDRI of the GCL were always lower than that of the INL regardless of the groups of mice examined, controls or conditional KOs. For example, the NNRI confirmed this difference between the layers in every genotype with an average NNRI of 3.74 ± 0.43 for the INL samples, whereas the GCL was significantly lower, 2.74 ± 0.25, $P < 0.011$. The average VDRI, although not significantly different ($P < 0.15$), followed a similar trend with a greater RI seen in the INL, 2.60 ± 0.61, than that for the GCL, 2.02 ± 0.28. This suggested that the mosaics of cholinergic ACs in the INL appeared more regular than the mosaics within the GCL, as has been reported previously.[19] Overall, these findings indicate that combined deletion of AP-2α and AP-2β transcription factors results in a significant disruption in the mosaic spacing of cholinergic ACs, specifically within the INL layer.

HCs Are Absent When AP-2α and AP-2β Are Deleted From the Retina

Earlier studies from our laboratory showed that combined deletion of AP-2α and AP-2β in the developing retina resulted in an absence of HCs in embryonic sections.[9] To further assess whether HCs are present in the postnatal DBL α/β KO mice in the current study, immunofluorescence labeling was performed using HC-type specific markers at P14. Calbindin, a calcium-binding protein that aids in calcium transport and is expressed by HCs located in the INL, was used as a marker for HCs. These studies demonstrated that double deletion of AP-2α and AP-2β resulted in an absence of calbindin staining in the retinal region in which HCs are typically present (Figs. 4C, 4D). To further assess HC deficiency, other markers were used, including neurofilament 160, which is found in the cytoskeleton of particular neurons (Figs. 4A, 4B); β-catenin, which is found in all neuronal processes and is essential for neuronal lamination (Figs. 4E, 4F); and Onecut-1,which is a precursor of HC development (Figs. 4G, 4H). All of these markers confirmed a complete loss of these interneurons in the retinas of the DBL α/β KO mutants that was not seen in single mutants or control littermates (Fig. 4 and data not shown).

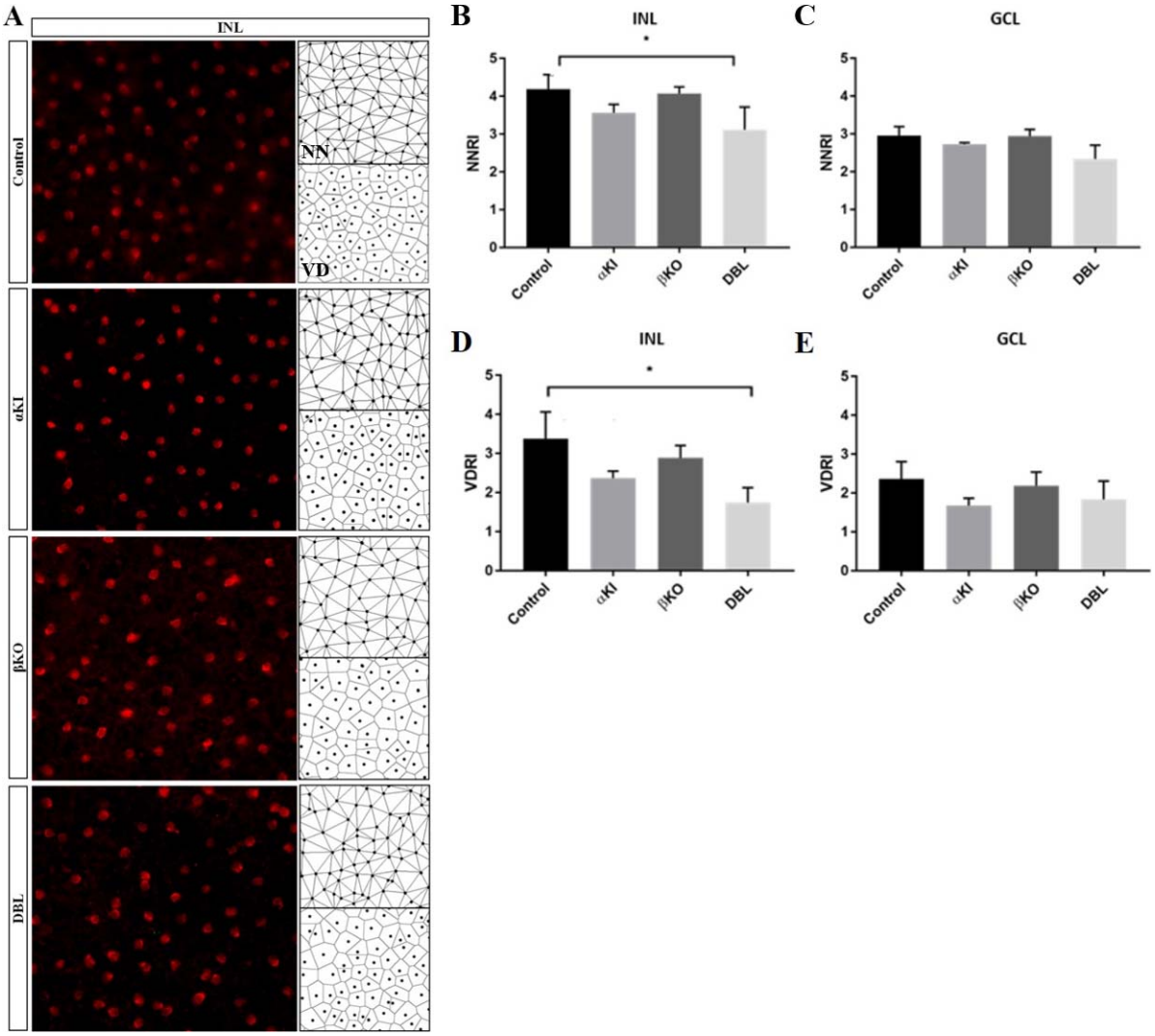

Figure 3. Decreased regularity in VD areas and NN distances in double-conditional KOs. (**A**) Retinal flat mounts (P50) were stained with ChAT (*red*) to visualize cholinergic ACs. NN and VD areas were determined using the FIJI version of ImageJ. (**B**) A marked decrease in NNRI was seen in the INL of DBL KO mice (3.12 ± 0.60) compared with controls (4.19 ± 0.39, $^*P < 0.03$). (**D**) A significant reduction in the VDRI in the INL of DBL KO mice (1.75 ± 0.38) compared with controls (3.38 ± 0.68) was observed ($^*P < 0.01$). No significant changes were seen in either RI in the GCL of either single KO or the double KO models (**C**, **E**). (Mean ± SD, four retinas per group; 1-way ANOVA with Bonferroni multiple comparisons test.) *Scale bar*: 100 μm.

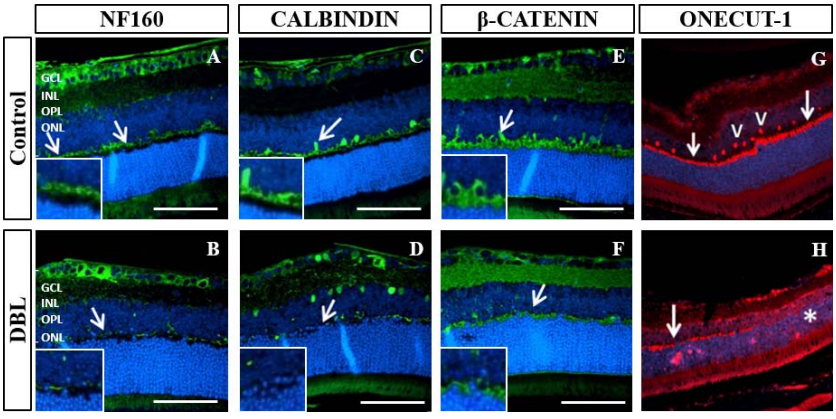

Figure 4. HC loss. Immunofluorescent analysis of P50 sagittal sections showing expression of HC markers in control and double KO mice. Control samples (**A**, **C**, **E**) depict expression within HCs in the OPL for neurofilament 160 (NF 160) (**A**), calbindin (**D**), β-catenin (*green*, *arrows*), and Onecut-1 (*red*), a marker of HC bodies (*arrowheads*) and their respective axons (*arrows*). Expression of these markers is absent in the periphery of the mutant retinas (*arrows*) (**B**, **D**, **F**, **H***), respectively. *Scale bars*: 100 μm.

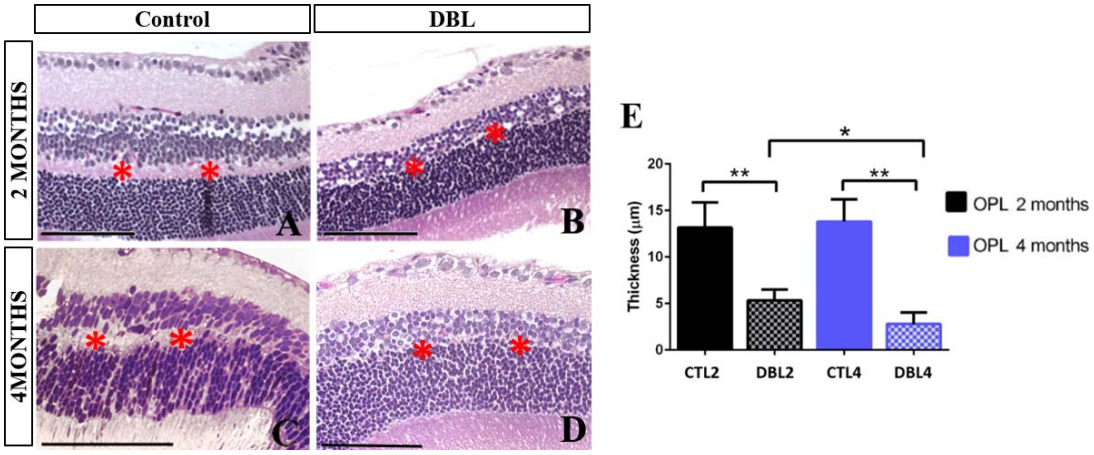

Figure 5. OPL diminishes over time. (**A**, **C**) Sagittal section of control retina, 2 months and 4 months, respectively, stained with H&E. All the nuclear and synaptic layers are intact, particularly the OPL (*). (**B**) Double KO retina, 2 months, the OPL has diminished significantly. (**D**) Double KO retina, 4 months. The OPL is practically absent, so that the border between the ONL and the INL is no longer distinguishable. (**E**) Examination of the thickness of the OPL revealed striking changes at 2 and 4 months, *black* and *blue bars*, respectively. The OPL of double KOs was significantly reduced at both time points when compared with age-matched controls (**$P < 0.001$). The OPL of the double KO also showed a significant reduction in width between 2 and 4 months of age (*$P < 0.05$). *Bars* represent the mean ± SEM of counts from three animals. *Scale bars*: 100 μm.

Abnormalities in the OPL in the Absence of AP-2α and AP-2β From the Retina

Another defect observed in the DBL α/β KO retina was a thinning of the OPL that was observed at 2 months of age and not seen in control littermates (Fig. 5). By 4 months, the OPL had completely disappeared, such that the outer nuclear layer (ONL) and INL appeared contiguous (Fig. 5D). Measurements of the OPL were recorded over the 2- and 4-month period, and post hoc analysis showed there was a significant decrease between the control and mutant retinas at both time points ($P < 0.001$) (Fig. 5). There was also a significant reduction in OPL thickness between the 2- and 4-month stage, $P < 0.05$ (Fig. 5), thereby demonstrating an overall reduction in this synaptic layer over time. Because the OPL is composed of PR terminals, and HC and BC processes, we surmised that a possible cause of the OPL thinning in the DBL α/β KO retinas was due to the loss of HCs, as demonstrated earlier, and their connections with the PRs. Indeed, HCs have been shown to be required for PR structure and viability and loss of HCs has shown to cause defects in synaptic connections between PRs and BCs. These specialized synaptic contacts, triadic ribbon synapses, are formed by a presynaptic PR ribbon, HC dendrites, and ON bipolar cell dendrites and are responsible for signal transmission between PRs, HCs, and BCs, to regulate PR output. In addition, structural changes in the classic triadic ribbon synapse have been observed in HC-ablated retinas.[27–31] Examination of these synaptic connections in the OPL by TEM allowed for the assessment of structural changes in the DBL α/β KO and we observed a complete absence of triad ribbon synapses of rod PRs consistent with a loss of HC processes (Fig. 6). Although the triad was absent, there were remnants of spherical ribbon-like structures present in these retinas (Fig. 6B, arrows), which are normally thin, long elongated structures (Fig. 6). Furthermore, there were observable defects in which PRs exhibited retracted axons (Fig. 6D, arrows). These abnormalities were not found in single αKI and βKO mutants (data not shown).

The Physiological Response to Light Is Altered by Loss of AP-2α and AP-2β From the Retina

As previously stated, correct visual processing depends on the proper arrangement and functionality of all retinal neurons. As we have shown herein, HCs are absent in adult DBL α/β KO as well as changes in the PRs and their synaptic connections. Proper PR synapse development is necessary to transduce visual stimuli to the HCs and ACs of the inner retina where the signals are further modulated, with disruption in this signal cascade causing changes in the functional response of the retina.[30,32,33] Thus, to determine the effect of these changes, dark-adapted full-field ERGs were used to compare αKI, βKO, and DBL α/β KO with control littermates. Control mice retinas were found to exhibit typical ERG waveforms characteristic of dark-adapted mice with a negative a-wave, depicting the hyperpolarization of rod PRs, and a positive b-wave representative of the depolarization of interneurons including HCs, BCs, and ACs (Fig. 7). As light intensity was increased, the response in control retinas also increased, with larger negative a-wave amplitudes and positive b-wave amplitudes observed. Both single conditional KOs, αKI and βKO, as well as DBL α/β KO mice showed a similar a-wave response to controls. In all cases, the amplitude negatively increased with brighter flashes of light, with an occasional significant difference occurring most likely due to interstrain variability (Fig. 7A).

In contrast, there were clear differences in the b-wave responses of these various mutant strains (Fig. 7B). First, in αKI mice, in which AP-2α is deleted from the retina, the b-wave amplitudes exhibit a trend similar to that seen in controls, increasing with light intensity. However, for the DBL α/β KOs, as light intensity was increased, the b-wave amplitude began to increase until a flash intensity of −1.108 log cd·s·m^{-2}, where it was found to significantly differ from controls ($P < 0.0003$). The b-wave amplitude then continued to significantly diverge from controls at all increasing flash intensities as the b-wave amplitude appeared to plateau ($P < 0.0001$) (Fig. 7B). Interestingly, the response of mice in which AP-2β was deleted from the retina showed an intermediate phenotype. Here, the b-wave amplitudes had a decreased response to light intensity compared with controls (Fig. 7B). The b-wave amplitude began to deviate from controls at a flash intensity of 0.875 log cd·s·m^{-2} and continued to be significantly different at increasing light intensities ($P < 0.0001$). However, unlike the DBL α/β KO mice where b-wave amplitudes appear to peak after a certain level of light intensity, the b-wave amplitudes in βKO mice continue to

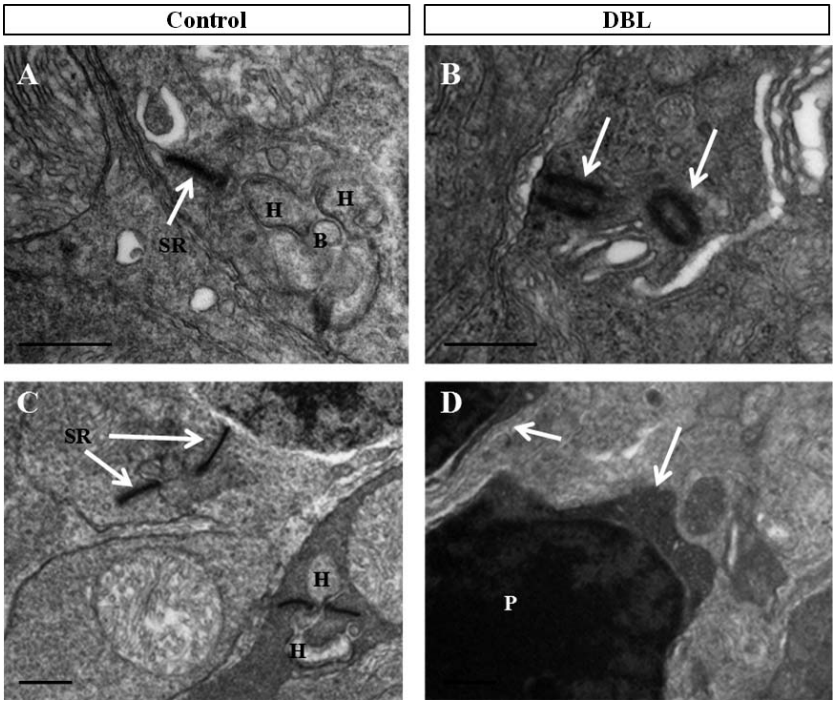

Figure 6. TEMs showing changes in the OPL. (**A**, **C**) Control retina, 4 months, exhibit typical ribbon synapses involving HCs and BCs. There are no observable defects in PR axon terminals. (**B**, **D**) At the same age, double mutants lack rod ribbon synapses, and instead sporadically display spherical-like ribbons in the outer plexiform of the retina (**B**, *arrows*), and exhibit axon retraction (**D**, *arrows*). SR, synaptic ribbon; H, horizontal cell; B, bipolar cells; P, photoreceptor. *Scale bars*: 500 µm.

increase but not to the same extent as controls or αKI mice. These findings suggest that downstream effects of deleting AP-2α and AP-2β from the retina may decrease the physiologic response to light, and that AP-2β may be more significant in this process than AP-2α.

Discussion

Retinogenesis is a complex process requiring precise coordination between intrinsic and extrinsic cues to regulate the development of RPCs into the neurons and glia necessary for

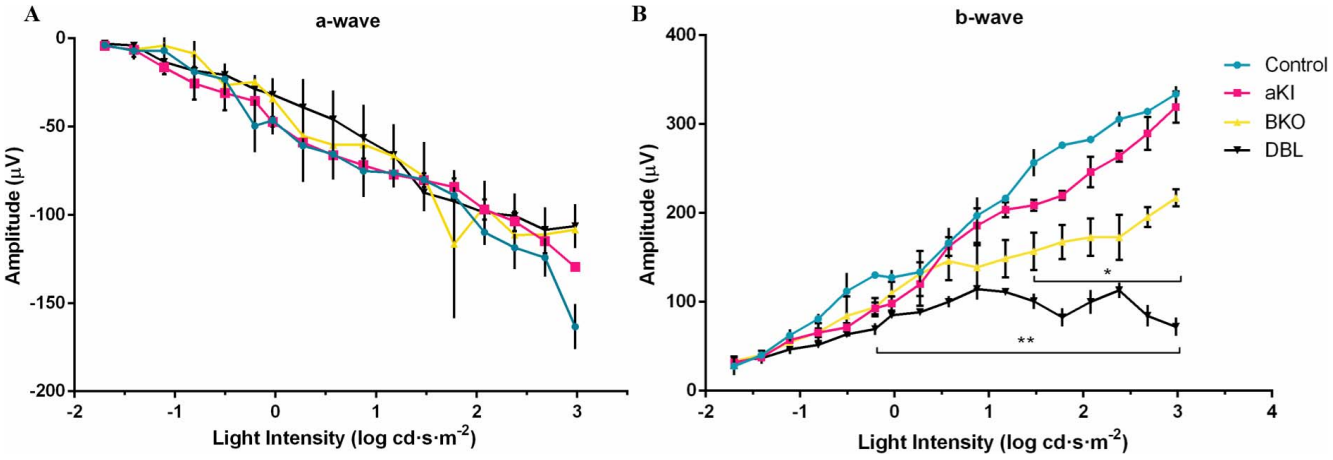

Figure 7. B-wave amplitudes are attenuated in double-conditional KO ERGs. (**A**) As flash intensities of light (504 nm) were increased, the a-wave decreased in a relative fashion, with flash intensity repeated measures yielding significantly different amplitudes ($F_{16,128} = 1626$, $P < 0.0001$). All groups tested, αKI (*pink*), βKO (*yellow*), and double KO mice (*black*), showed a similar pattern to that seen in control mice (*blue*). The hyperpolarization of PRs, as represented by this a-wave, appears to be maintained regardless of deletion of AP-2α, AP-2β, or AP-2α/β from the retina. No significant deviance from controls was observed. (Mean ± SD, three eyes analyzed per group, 2-way repeated-measures ANOVA with Tukey's HSD post hoc analysis between genotypes.) (**B**) B-wave amplitudes are attenuated in double-conditional KO ERGs. As flash intensities increased, the b-wave in control mice increases proportionately (*blue*), with flash intensity repeated measures yielding significantly different amplitudes ($F_{16,128} = 1626$, $P < 0.0001$). αKI mice show a similar positive correlation between light intensity and b-wave amplitude as controls. Beginning at a flash intensity of 0.875 log cd·s·m^{-2}, βKO b-wave amplitudes continue to be significantly different from controls ($P < 0.0001$). In DBL KO mice, the depolarization of cells in the inner retina, as measured by the b-wave, appear to be severely affected in the DBL KO when compared with all other mice studied. At a flash intensity of −1.108 log cd·s·m^{-2}, the b-wave amplitude of the DBL KO mice is significantly different from controls ($P < 0.0003$) and continue to significantly deviate from control values at subsequent increasing light intensities ($P < 0.0001$). (Mean ± SD, three eyes for each group analyzed, 2-way repeated-measures ANOVA with Tukey's HSD post hoc analysis between genotypes.)

vision. Regulatory factors, such as transcription factors, have been shown to affect cell fate determination, spatial arrangement, and the synaptic connections between homo- and heterotypic cells of the retina. Our laboratory has previously shown that AP-2 transcription factors, in particular AP-2α and AP-2β, exhibit overlapping expression in the AC and HC populations of the embryonic murine retina, continuing into the postnatal stages.[9,10] In addition, we have shown that double deletion of AP-2α and AP-2β from the retina of embryonic mice results in an absence of HCs and abnormal cellular arrangement of cholinergic ACs as was observed in histological sections immunolabeled with SOX2 and ISL1/2.[9] Because these mutants did not survive beyond birth, the current study was carried out to examine how double deletion of AP-2α and AP-2β affects retinogenesis postnatally. Indeed, postnatal mice lacking both AP-2α and AP-2β (DBL α/β KO) in the retina exhibited loss of HCs, aberrant AC mosaics, and altered sublamination, which culminated in abnormal retinal function, as determined by ERG.

We have shown herein that on deletion of both AP-2α and AP-2β, the AC population number was not affected. For all AC classes examined, GABAergic, glycinergic, and the subpopulation of cholinergic ACs, no significant decreases in AC numbers were observed in the DBL α/β KOs. This was also found to be the case in embryonic staged double mutants examined earlier.[9] Together these results suggest that AP-2α and β are not directly involved in the genesis of ACs. Our findings are in contrast to a recent study that indicated that small interfering RNA knockdown of AP-2α/AP-2β expression ablated all AC populations.[34] The contrariety of our studies with these findings may be due to the different techniques used to remove the expression of AP-2α and AP-2β from the retina. In our study, we used a genetic approach to conditionally delete both genes, whereas Jin et al.[34] used electroporation techniques to transfect *Tfap2a* and *Tfap2b* small hairpin RNAs (shRNAs) into the retina to knock down expression of AP-2α and AP-2β. Due to the similarity in sequence of the AP-2 family of genes,[15] it is feasible that binding of the shRNA to other family members, such as AP-2γ or AP-2ε, may have occurred. Both AP-2γ and AP-2ε have previously been shown to exhibit overlapping expression with AP-2α and AP-2β in ACs.[9,35] Thus, downregulation of these additional AP-2 family member may have caused an alteration in AC numbers.[34] Additional investigation of the role of other AP-2 family members in retinogenesis will therefore be important to further determine how they may, together, control AC formation.

Although we did not observe a change in AC populations, our findings did reveal that in the absence of both AP-2α and AP-2β mice exhibited a significant difference in AC mosaics as revealed by both NN distances and VD areas analyses, methods to measure retinal mosaics, and spacing of homotypic cells.[19,36] The cholinergic ACs in the INL of mice exhibit a distinctly regular distribution, and their patterning is one of the most well-studied mosaics in the central nervous system.[37] Typically, during retinal development there is a mutual repulsion between homotypic cells proximal to one another, which creates exclusion zones, dispersing the neurons throughout the retina.[38,39] The molecular cues that regulate and maintain this cellular positioning remain poorly understood. Recently, pituitary tumor transforming gene 1 (Pttg1) expression has been correlated with regular retinal mosaic, with a significant decrease in the regulatory indexes in retinas where Pttg1 expression is lost.[40] As well, a small number of studies have examined potential regulators of AC spacing and arrangement, including the adhesion protein podocalyxin, which has been implicated to play a role in the growth and migration of neuronal processes, MEGF10, which has been shown to aid in recognition and repulsion between homotypic cells, and Down syndrome cell adhesion molecule (Dscam) which has been shown to prevent cell-cell adhesions that allow dendrites to migrate to their appropriate destination within the retina.[41–44] Because the AP-2 genes, and in particular AP-2α, can directly regulate the expression of cell-cell adhesion family members, such as the cadherins, it is feasible that they may control the mosaics through this type of regulation. For example, AP-2 directly regulates E-cadherin expression in the lens[45] and N-cadherin upregulation in corneal cells where AP-2α is overexpressed.[46] Many members of the cadherin family are found in the retina, including R-cadherin; cadherins 6, 7, and 11; and protocadherin.[47] Thus, it is possible that these retinal-specific cadherins also may be under transcriptional regulation by AP-2α and AP-2β.

Unlike the DBL α/β KOs, the single αKI and βKO mice in this study did not exhibit significant differences in AC arrangement as determined by the NNRI or VDRI, suggesting that deletion of AP-2α or AP-2β alone was not sufficient to create changes in the mosaic patterning of cholinergic ACs. AP-2α and AP-2β have been shown in both embryonic and adult mice to have similar expression patterns in the AC population.[9] AP-2 transcription factors also can act as homo- or heterodimers with one another to regulate the expression of target genes, and thus family members are able to compensate for one another to a certain extent.[9] This is likely to be the case for AP-2α and AP-2β in both AC mosaics, as well as for HC cell genesis in the retina. Interestingly, in all mice examined, both single and DBL mutants, the displaced cholinergic ACs residing in the GCL consistently appeared more irregular than those in the INL. This disparity between the mosaic of the GCL and INL is well documented in several mouse lines and it has been proposed to be a natural outcome of remodeling of the GCL during development.[19] The cholinergic AC mosaics in the INL are unaffected by the developmental remodeling, and this may explain why it was easier to detect an irregular pattern in this layer of the retina in the DBL conditional KOs.

During retinal development, horizontal cell processes recruit synaptic ribbons to PRs by creating sites of contact at the synapse. This contact and recruitment then promotes a second HC process to arrive at the synapse, followed by the addition of an ON bipolar cell dendrite.[48] Together, this complex forms a synaptic ribbon triad. We examined whether the loss of HCs affected this structure and discovered a complete absence of the ribbon triad in DBL α/β KO mice with only remnant-like spherically shaped ribbons evident. This absence was not observed in single mutants or littermate controls. The absence of the triad has been extensively recorded in studies examining HC-ablated retinas. For example, these changes resembled effects caused by genetic mutations of HCs, such as the loss of Onecut-1,[31] other mutations induced by toxins such as diphtheria,[30] and effects caused by the loss of PR synaptic proteins, such as CaBP4[27] and bassoon.[29] Thus, the absence of the triad in our mutants was likely related to the lack of HCs.

Because the development of PR synapse formation is integral to transmission of signals from the rods to BCs and subsequently to the inner retina, we used ERG to measure the retinal response to light in the mutant mice. The complex electrical circuitry of the retina is susceptible to signal transmission inhibition detectable by the recorded ERG response.[48] The a-wave measures the functional response of PRs to a light stimulus.[49] The recordings from single αKI and βKOs, and DBL α/β KO had no observable deviations from the a-wave recorded in control mice, suggesting the hyperpolarization of dark-adapted PRs in response to light was unaffected by loss of AP-2α/AP-2β from the retina. The signal-processing

Investigative Ophthalmology & Visual Science

response of HC, AC, and BC interneurons post-synaptic to the PRs is recorded as the b-wave in ERGs.[30,32] Here, in contrast to the similarities in a-wave amplitude response, transmission of the PR signal forward to the inner retina was altered by the deletion of AP-2α and AP-2β, resulting in a decrease in b-wave amplitudes. In the DBL α/β KO, we observed a large decrease in the amplitudes of b-waves recorded, as expected from the PR synapse remodeling and loss of HCs from the retina. Interestingly, the b-wave amplitudes of single βKO mice decreased significantly compared with controls, although not to the same extent as those in the DBL α/β KO, whereas AP-2α deletion appeared to have little influence on the ERG response. We have shown previously that although embryonic HCs express both AP-2α and AP-2β, in the adult retina HCs exclusively express AP-2β.[9] Thus, the loss of AP-2β expression in the single conditional βKO in adults may have affected this population more significantly and thereby altered signal transmission from PRs. Other interneurons of the retina, such as cholinergic ACs, may also contribute to the b-wave response, with changes in the depolarization of cholinergic ACs known to reduce b-wave amplitudes in dark-adapted mice.[33] However, as we have shown while the mosaic arrangement of cholinergic ACs was affected, the population of these cells did not change. Thus, whether the disorganization of AC mosaics had any effect on the b-wave amplitude is not known. Oscillatory potentials (OPs) appear as four to six small waves on the rising phase of the ERG b-wave. Although the specific cellular origin of OPs is still debated, there is strong evidence that GABAergic neurons and synaptic interactions are key elements in this response.[50] Analyzing these OPs could provide a more confident correlation between of the functional response in the DBL KO mice with irregularities in their AC mosaic patterning.

Overall, this study has shown that although conditional double deletion of both AP-2α and AP-2β did not affect the birth of ACs during retinogenesis, it did affect the regulation of AC mosaic formation. The mechanism by which this was disrupted is not known, but may have occurred through a loss of regulation in expression of cell adhesion molecules involved in homotypic interactions that determine AC soma and neurite spacing. Due to the changes in neuronal arrangement of ACs and loss of HCs in the DBL α/β KO, the electrophysiological response to light was compromised with signals being processed less effectively and efficiently, limiting the output of PRs on the interneurons and the signals relayed from the GCs to the brain. These findings illustrate the importance of precise cooperative transcriptional regulation by AP-2α and AP-2β of interneuron patterning during retinal development.

Acknowledgments

The authors thank Reinhard Buettner (University Hospital Cologne, Center for Integrated Oncology Kerpener Strasse) for generously providing mice carrying the Tfap2b-null allele. The monoclonal anti-AP-2α (3B5) monoclonal antibody was developed by Trevor Williams and obtained from the Developmental Studies Hybridoma Bank (created by the National Institute of Child Health and Human Development of the National Institutes of Health) and maintained at The University of Iowa, Department of Biology, Iowa City, Iowa, United States.

Supported by the National Eye Institute/National Institutes of Health Grant EY025789 (JAWM), The Foundation Fighting Blindness (JAWM), and National Institute of Dental and Craniofacial Research Grant RO1 DE12728 (TW).

Disclosure: **E.A. Hicks**, None; **M. Zaveri**, None; **P.A. Deschamps**, None; **M.D. Noseworthy**, None; **A. Ball**, None; **T. Williams**, None; **J.A. West-Mays**, None

References

1. Livesey FJ, Cepko CL. Vertebrate neural cell-fate determination: lessons from the retina. *Nat Rev Neurosci*. 2001;2:109–118.
2. Marquardt T. Transcriptional control of neuronal diversification in the retina. *Prog Retin Eye Res*. 2003;22:567–577.
3. Cepko CL. The roles of intrinsic and extrinsic cues and bHLH genes in the determination of retinal cell fates. *Curr Opin Neurobiol*. 1999;9:37–46.
4. Kageyama R, Ohtsuka T, Hatakeyama J, Ohsawa R. Roles of bHLH genes in neural stem cell differentiation. *Exp Cell Res*. 2005;306:343–348.
5. Li S, Mo Z, Yang X, Price SM, Shen MM, Xiang M. Foxn4 controls the genesis of amacrine and horizontal cells by retinal progenitors. *Neuron*. 2004;43:795–807.
6. Fujitani Y, Fujitani S, Luo H, et al. Ptf1a determines horizontal and amacrine cell fates during mouse retinal development. *Development*. 2006;133:4439–4450.
7. Bassett EA, Pontoriero GF, Feng W, et al. Conditional deletion of activating protein 2alpha (AP-2alpha) in the developing retina demonstrates non-cell-autonomous roles for AP-2alpha in optic cup development. *Mol Cell Biol*. 2007;27:7497–7510.
8. West-Mays JA, Zhang J, Nottoli T, et al. AP-2alpha transcription factor is required for early morphogenesis of the lens vesicle. *Dev Biol*. 1999;206:46–62.
9. Bassett EA, Korol A, Deschamps PA, et al. Overlapping expression patterns and redundant roles for AP-2 transcription factors in the developing mammalian retina. *Dev Dyn*. 2012;241:814–829.
10. Bassett EA, Williams T, Zacharias AL, Gage PJ, West-Mays JA. AP-2alpha knockout mice exhibit optic cup patterning defects and failure of optic stalk morphogenesis. *Hum Mol Genet*. 2010;19:1791–1804.
11. Bisgrove DA, Godbout R. Differential expression of AP-2alpha and AP-2beta in the developing chick retina: repression of R-FABP promoter activity by AP-2. *Dev Dyn*. 1999;214:195–206.
12. Bisgrove DA, Monckton EA, Godbout R. Involvement of AP-2 in regulation of the R-FABP gene in the developing chick retina. *Mol Cell Biol*. 1997;17:5935–5945.
13. Li X, Monckton EA, Godbout R. Ectopic expression of transcription factor AP-2delta in developing retina: effect on PSA-NCAM and axon routing. *J Neurochem*. 2014;129:72–84.
14. Li X, Gaillard F, Monckton EA, et al. Loss of AP-2delta reduces retinal ganglion cell numbers and axonal projections to the superior colliculus. *Mol Brain*. 2016;9:62.
15. Eckert D, Buhl S, Weber S, Jager R, Schorle H. The AP-2 family of transcription factors. *Genome Biol*. 2005;6:246.
16. Zhang J, Hagopian-Donaldson S, Serbedzija G, et al. Neural tube, skeletal and body wall defects in mice lacking transcription factor AP-2. *Nature*. 1996;381:238–241.
17. Schorle H, Meier P, Buchert M, Jaenisch R, Mitchell PJ. Transcription factor AP-2 essential for cranial closure and craniofacial development. *Nature*. 1996;381:235–238.
18. Reese BE, Galli-Resta L. The role of tangential dispersion in retinal mosaic formation. *Prog Retin Eye Res*. 2002;21:153–168.
19. Whitney IE, Keeley PW, Raven MA, Reese BE. Spatial patterning of cholinergic amacrine cells in the mouse retina. *J Comp Neurol*. 2008;508:1–12.
20. Brewer S, Jiang X, Donaldson S, Williams T, Sucov HM. Requirement for AP-2alpha in cardiac outflow tract morphogenesis. *Mech Dev*. 2002;110:139–149.
21. Moser M, Pscherer A, Roth C, et al. Enhanced apoptotic cell death of renal epithelial cells in mice lacking transcription factor AP-2beta. *Genes Dev*. 1997;11:1938–1948.

22. Marquardt T, Ashery-Padan R, Andrejewski N, Scardigli R, Guillemot F, Gruss P. Pax6 is required for the multipotent state of retinal progenitor cells. *Cell*. 2001;105:43–55.
23. Brewer S, Feng W, Huang J, Sullivan S, Williams T. Wnt1-Cre-mediated deletion of AP-2alpha causes multiple neural crest-related defects. *Dev Biol*. 2004;267:135–152.
24. Vaney DI. The mosaic of amacrine cells in the mammalian retina. *Progress in Retinal Research*. 1990;9:49–100.
25. Galli-Resta L, Resta G, Tan S-S, Reese BE. Mosaics of Islet-1-expressing amacrine cells assembeled by short range cellular interactions. *J Neurosci*. 1997;17:7831–7838.
26. Lin YP, Ouchi Y, Satoh S, Watanabe S. Sox2 plays a role in the induction of amacrine and Müller glial cells in mouse retinal progenitor cells. *Invest Ophthalmol Vis Sci*. 2009;50:68–74.
27. Haeseleer F, Imanishi Y, Maeda T, et al. Essential role of Ca2+-binding protein 4, a Cav1.4 channel regulator, in photoreceptor synaptic function. *Nat Neurosci*. 2004;7:1079–1087.
28. Chang B, Heckenlively JR, Bayley PR, et al. The nob2 mouse, a null mutation in Cacna1f: anatomical and functional abnormalities in the outer retina and their consequences on ganglion cell visual responses. *Vis Neurosci*. 2006;23:11–24.
29. Specht D, Tom Dieck S, Ammermuller J, Regus-Leidig H, Gundelfinger ED, Brandstatter JH. Structural and functional remodeling in the retina of a mouse with a photoreceptor synaptopathy: plasticity in the rod and degeneration in the cone system. *Eur J Neurosci*. 2007;26:2506–2515.
30. Sonntag S, Dedek K, Dorgau B, et al. Ablation of retinal horizontal cells from adult mice leads to rod degeneration and remodeling in the outer retina. *J Neurosci*. 2012;32:10713–10724.
31. Wu F, Li R, Umino Y, et al. Onecut1 is essential for horizontal cell genesis and retinal integrity. *J Neurosci*. 2013;33:13053–13065.
32. Dick O, tom Dieck S, Altrock WD, et al. The presynaptic active zone protein bassoon is essential for photoreceptor ribbon synapse formation in the retina. *Neuron*. 2003;37:775–786.
33. Elgueta C, Vielma AH, Palacios AG, Schmachtenberg O. Acetylcholine induces GABA release onto rod bipolar cells through heteromeric nicotinic receptors expressed in A17 amacrine cells. *Front Cell Neurosci*. 2015;9:6.
34. Jin K, Jiang H, Xiao D, Zou M, Zhu J, Xiang M. Tfap2a and 2b act downstream of Ptf1a to promote amacrine cell differentiation during retinogenesis. *Mol Brain*. 2015;8:28.
35. Jain S, Glubrecht DD, Germain DR, Moser M, Godbout R. AP-2ε expression in developing retina: contributing to the molecular diversity of amacrine cells. *Sci Rep*. 2018;8:3386.
36. Raven MA, Eglen SJ, Ohab JJ, Reese BE. Determinants of the exclusion zone in dopaminergic amacrine cell mosaics. *J Comp Neurol*. 2003;461:123–136.
37. Whitney IE, Keeley PW, St John AJ, Kautzman AG, Kay JN, Reese BE. Sox2 regulates cholinergic amacrine cell positioning and dendritic stratification in the retina. *J Neurosci*. 2014;34:10109–10121.
38. Eglen SJ, van Ooyen A, Willishaw DJ. Lateral cell movement driven by dendritic interactions is sufficient to form retinal mosaics. *Network*. 2000;11:103–118.
39. Eglen SJ, Willishaw DJ. Influence of cell fate mechanisms upon retinal mosaic formation: a modelling study. *Development*. 2002;129:5399–5408.
40. Keeley PW, Zhou C, Lu L, Williams RW, Melmed S, Reese BE. Pituitary tumor-transforming gene 1 regulates the patterning of retinal mosaics. *Proc Natl Acad Sci U S A*. 2014;111:9295–9300.
41. Fuerst PG, Koizumu M, Masland RH, Burgess RW. Neurite arborization and mosaic spacing in the mouse retina require DSCAM. *Nature*. 2008;451:470–474.
42. Fuerst PG, Bruce F, Tian M, et al. DSCAM and DSCAML1 function in self-avoidance in multiple cell types in the developing mouse retina. *Neuron*. 2009;64:484–497.
43. Keeley PW, Sliff BJ, Lee SC, et al. Neuronal clustering and fasciculation phenotype in Dscam- and Bax-deficient mouse retinas. *J Comp Neurol*. 2012;520:1349–1364.
44. Kay JN, Chu MW, Sanes JR. MEGF10 and MEGF11 mediate homotypic interactions required for mosaic spacing of retinal neurons. *Nature*. 2012;483:465–469.
45. Pontoriero GF, Deschamps P, Ashery-Padan R, et al. Cell autonomous roles for AP-2alpha in lens vesicle separation and maintenance of the lens epithelial cell phenotype. *Dev Dyn*. 2008;237:602–617.
46. West-Mays JA, Sivak JM, Papagiotas SS, et al. Positive influence of AP-2alpha transcription factor on cadherin gene expression and differentiation of the ocular surface. *Differentiation*. 2003;71:206–216.
47. Honjo M, Tanihara H, Suzuki S, Tanaka T, Honda Y, Takeichi M. Differential expression of cadherin adhesion receptors in neural retina of the postnatal mouse. *Invest Ophthalmol Vis Sci*. 2000;41:546–551.
48. Wassle H. Parallel processing in the mammalian retina. *Nat Rev Neurosci*. 2004;5:747–757.
49. Pinto LH, Invergo B, Shimomura K, Takahashi JS, Troy JB. Interpretation of the mouse electroretinogram. *Doc Ophthalmol*. 2007;115:127–136.
50. Ramsey DJ, Ripps H, Qian H. An electrophysiological study of retinal function in the diabetic female rat. *Invest Ophthalmol Vis Sci*. 2006;47:5116–5124.

Investigative Ophthalmology & Visual Science